PROPERTIES OF SUPPORTED RHODIUM CATALYSTS FOR STEAM DEALKYLATION OF TOLUENE

Ro Yong Zun*, Helena Davidová, Jaroslava Polednová, Květa Jirátová and Petr Schneider

Institute of Chemical Process Fundamentals
Czechoslovak Academy of Sciences, 165 02 Prague 6-Suchdol

Received September 10th, 1987

The effect of modification of γ-alumina support by Cr_2O_3 on physical and catalytic properties of supported rhodium catalysts was investigated. Various techniques were used for characterization of catalysts: porosimetry, diffusion and permeation measurements, determination of surface OH groups, temperature-programmed reduction and catalytic behaviour in steam dealkylation of toluene. Using the transport parameters determined for pelleted catalysts the effect of internal diffusion on the reaction was predicted and compared with experiments.

Steam dealkylation of toluene represents a very interesting heterogeneously catalyzed reaction producing benzene, in which hydrogen is not consumed but produced.

$$C_6H_5CH_3 + H_2O \rightarrow C_6H_6 + CO + 2\,H_2 \qquad (A)$$

Simultaneously with this demanded reaction, fast conversion of water-gas takes place.

$$CO + H_2O \rightarrow CO_2 + H_2 \qquad (B)$$

The amount and quality of the formed hydrogen is lowered by the carbon monoxide methanation.

$$CO + H_2 \rightarrow CH_4 + H_2O \qquad (C)$$

In the presence of unsufficiently selective catalysts, several other reactions can take place:
hydrodealkylation of toluene to benzene and methane,

$$C_6H_5CH_3 + H_2 \rightarrow C_6H_6 + CH_4 \qquad (D)$$

* On leave from the Institute of Chemistry, Hamhung, DPR Korea.

splitting of toluene to carbon monoxide and hydrogen

$$C_6H_5CH_3 + 7\,H_2O \rightarrow 7\,CO + 11\,H_2 \quad (E)$$

or to carbon and hydrogen.

$$C_6H_5CH_3 \rightarrow 7\,C + 4\,H_2 \quad (F)$$

In the steam dealkylation of toluene, metals of the VIII periodic group are active[1]. The following selectivities to benzene were observed[2] for metals: Pt, Pd 97–98%; Ir 88%; Rh 81%; Ni 59%; Ru 53%; Co 51%. These values are significantly lower than for hydrodealkyation of toluene where 90 to 100% benzene can be obtained[3–5]. For toluene steam dealkylation the recommended and most frequently studied metal is rhodium[6–10].

Activity, selectivity and stability of the catalyst can be changed by the support used[2,11–13]: Rh/γ-Al_2O_3 catalyst is the most active but the least stable. According to Duprez[3] selectivities to benzene of various supported rhodium catalysts decrease in the order: $TiO_2 > Cr_2O_3 > Al_2O_3 > SiO_2$. Because of the good selectivity and stability, Kochloefl[13] considers Rh/Cr_2O_3 as the industrially most advantageous catalyst despite its lower activity.

The aim of this work was to describe the effect of Cr_2O_3 addition to γ-Al_2O_3 support of rhodium catalysts on the physical properties of the resulting catalysts and on their activity and selectivity. Samples of rhodium catalysts supported on mechanical mixtures of Cr_2O_3 and γ-Al_2O_3 were prepared and characterized by porosimetry, temperature-programmed reduction and by titration with dimethylzinc tetrahydrofuranate (determination of the concentration of surface OH groups). Parameters characterizing the mass transport in pores of pelleted samples were determined by combination of permeation and diffusion measurements. Catalytic activity and selectivity of the reduced samples was tested in steam dealkylation of toluene at atmospheric pressure and 460°C.

EXPERIMENTAL

Chemicals. Toluene p.a., chromium(III) oxide p.a. (Lachema, Brno, Czechoslovakia); aluminium hydroxide (Pural S, Condea Chemie, F.R.G.); rhodium chloride p.a. (Koch–Light Laboratories, England); nitrogen, hydrogen (Technoplyn, Kyje, Czechoslovakia); redistilled water.

Catalysts. Hand-mixed intimate mixtures of required amounts of aluminium hydroxide and chromium(III) oxide were pelleted under identical pressure in a laboratory press. Cylindrical pellets (diameter × height = 5 × 5 mm) were impregnated by KNO_3 solution to the content 1·6 wt. % K, dried and calcined 4 h at 600°C under the flow of air-steam mixture. After calcination, a part of the pellets of each sample was crushed and sieved out to the size 0·3–0·5 mm. Small grains as well as pellets were impregnated by $RhCl_3$ solution to 1·5 wt. % Rh, dried 4 h at 120°C and calcined 3 h at 550°C.

Porous structure. Total pore volume, pore size distribution, and apparent (pellet) density were determined by mercury porosimetry (AutoPore 9 200, Micromeritics, U.S.A.). Skeletal density was measured by helium pycnometry (AutoPycnometer 1 320, Micromeritics, U.S.A.). Specific surface area was evaluated from nitrogen adsorption at −195°C by the BET method (DigiSorb 6 200, Micromeritics, U.S.A.).

Transport parameters of catalyst pellets were obtained from combination of permeation and counter-current binary diffusion measurements[14] and RTG *analysis* was carried out on Difractograph Phillips with CuKα radiation source.

Temperature-programmed reduction. The sample (0·05—0·25 g) was placed in a glass reactor (internal diameter 4 mm) through which the H_2–N_2 mixture (0·95 l (H_2)/h, 0·69 l(N_2)/h) was passed. Temperature was increased linearly with the rate 20 K/min. Water formed during reduction was freezed out and the change in the composition of the outlet gas mixture was followed by a thermal conductivity detector.

Number of surface OH *groups* on the catalyst supports were determined by titration with dimethylzinc tetrahydrofuranate[15]. The support (0·02—0·05 g) was heated for 3 h in hydrogen stream at temperatures in the range 300—500°C and after cooling to room temperature, surface OH groups were titrated by pulses of the organometallic agent in chromatographic arrangement. The number of OH groups was determined from the amount of methane formed.

Catalyst activity was determined in a laboratory integral glass flow reactor. Toluene and water was fed separately by linear feed devices into a preheater kept at 120°C; the preheated gas mixture then entered the catalytic reactor. The stream leaving the reactor was cooled down to 0°C and the accumulated aqueous and organic phases were separated. The volume of noncondensed gases was determined in a gas burette. Every 30 min the liquid products were weighed and the composition of the gaseous products as well as of both liquid phases was determined by gas chromatography. Gaseous products: column 3 m × 3 mm (Porapak N); carrier gas argon; temperature 100°C; thermal conductivity detector. Liquid products: column 3 m × 3 mm (95% Chromosorb W + 5% mixture of Bentone 34 and dinonylsebacate (2 : 1)); carrier gas hydrogen; temperature 72°C; flame ionization detector. Because of the chemical similarity of benzene and toluene, their area fractions in chromatograms were taken as weight fractions.

Prior to reaction, catalysts were reduced 2 h at 460°C in the stream of H_2–N_2 mixture (molar ratio 1 : 1, mixture space velocity 100 $cm^3/h\ g_{cat}$). Reaction conditions: pressure 0·1 MPa, temperature 460°C, toluene space velocity F/W = 0·025—0·2 mol/h g_{cat}, molar ratio water/ /toluene in the feed 5/1. Initial reaction rates of toluene were determined as slopes of the dependence: toluene conversion (x_T) vs W/F at $W/F = 0$. Integral selectivity of benzene, S_B, was calculated as

$$S_B = n_B/(n_T^0 - n_T)\,, \qquad (1)$$

where n_B and n_T are the molar amounts of benzene and toluene, resp., in condensed products after 30 min of reaction and n_T^0 is the amount of toluene fed into the reactor during this time. Similarly, parameters $P(i)$ characterizing formation of gaseous reaction products i (i = hydrogen, methane, carbon monoxide, carbon dioxide, resp.) are defined as

$$P(i) = n_i/(n_T^0 - n_T)\,. \qquad (2)$$

RESULTS AND DISCUSSION

Catalyst composition. Results obtained from electron microprobe (EDX) are given in Table I. It is evident that composition differences between grains and pellets are small; it is believed that these differences will not affect the activity and selectivity substantially.

RTG *analysis* of supports provided diffraction spectra in which only lines of imperfectly crystallised aluminium oxide were distinguished. Because of the low amount of chromium(III) oxide in the mixed supports none of the supports exhibited lines of chromium(III) oxide.

Textural properties of the supports depend on the amount of Cr_2O_3 (Table II). Surface area of pure Cr_2O_3 is one twentieth of that for γ-Al_2O_3 and its skeletal density is twice higher. Surface areas of mixed oxides as well as their apparent densities depend linearly on weight fraction of the mixture constituents. Pore size distributions of the prepared samples are shown in Fig. 1. Pure γ-Al_2O_3 has bidisperse pore

TABLE I
Catalyst composition (wt. %)

Cr_2O_3 in support wt. %	Small grains			Pellets		
	Cr_2O_3	K_2O	Rh	Cr_2O_3	K_2O	Rh
0	0	1·8	1·6	0	1·4	1·5
10	10·5	1·6	1·8	11·2	1·3	1·8
16	16·0	1·7	1·8	16·3	1·6	1·7
100	96·4	2·0	1·6	96·8	1·7	1·5

TABLE II
Textural properties of supports

Cr_2O_3 in support wt. %	Specific surface[a] m^2/g	Density g/cm^3		Porosity %		Most frequent pore radii[b], nm	
		apparent[c]	skeletal[d]	total	macropores[b]	mesopores	macropores
0	133	1·293	3·138	58·8	11·6	5	160
10	120	1·278	3·121	59·1	13·2	5	260
16	114	1·388	3·368	58·8	15·2	5	330
100	6·8	2·46	5·355	54·1	54·1	—	260

[a] BET; [b] from combination of mercury porosimetry and adsorption of nitrogen; [c] pycnometrically with mercury; [d] pycnometrically with helium.

structure (mesopore radius about 5 nm, macropore radius 160 nm), pure Cr_2O_3 is monodisperse with macropores radii about 260 nm. Pore size distributions of mixed supports are essentially summation curves of the pore size distributions of the mixture constituents, weighed by the fractions of constituents in the mixture.

Transport parameters of catalyst pellets with different amounts of Cr_2O_3 in the support are given in Table III. From the comparison of transport pore radii, $\bar{r}$, and

TABLE III

Transport parameters ($\bar{r}$ — mean transport pore radius, ψ — porosity/tortuosity of transport pores) of catalyst pellets

Cr_2O_3 in support, wt. %	$\bar{r}$ nm	$\psi \cdot 10^2$
0	160	4·65
10	161	5·86
16	225	5·82

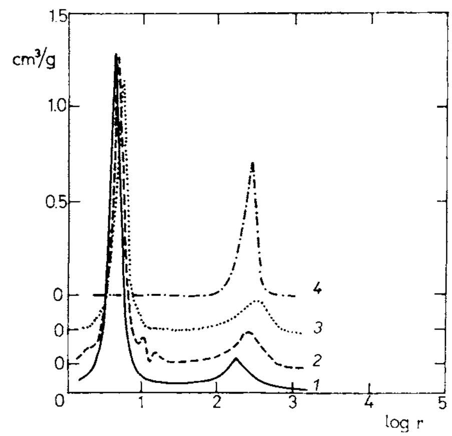

FIG. 1

Pore size distributions of supported catalysts. Amount of Cr_2O_3 in support (wt. %): *1* 0%; *2* 10%; *3* 16%; *4* 100%

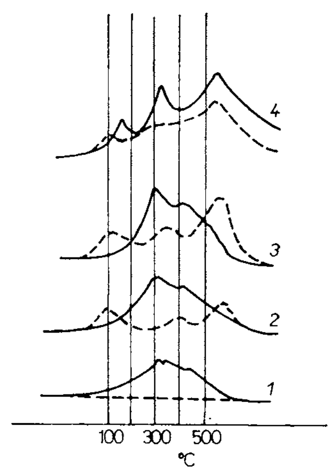

FIG. 2

Temperature-programmed reduction of rhodium catalysts (——) and corresponding supports (– – –). Amount of Cr_2O_3 in support (wt. %): *1* 0%; *2* 10%; *3* 16%; *4* 100%

pore size distributions (Fig. 1, Table II) it follows that macropores are responsible for mass transport in the porous pellets. Parameter ψ represents the effective porosity of transport pores; on assuming that all macropores are effective in the mass transport (i.e. porosity of macropores (Table II) equals the porosity of transport pores) we obtain for tortuosities of transport pores in catalysts with 0%, 10%, and 16% Cr_2O_3 in the support the following values: 2·49, 2·25, and 2·61. Tortuosities of this magnitude are often found for industrial catalysts[16].

Temperature-programmed reduction. Results of temperature-programmed reduction of supported rhodium catalysts and corresponding supports are shown in Fig. 2. Pure chromium(III) oxide and all supports which contain Cr_2O_3 start to be reduced at temperatures below 100°C, practically at 25°C. The reason is, obviously, the presence of very easily reducible chromium(VI) oxide which is formed in the surface layers of chromium(III) oxide during its calcination in oxygen containing atmosphere.

The presence of Cr(VI) in surface layers of Cr_2O_3/Al_2O_3 catalyst/supports was proved by photoelectron spectroscopy[17]. According to Grünert and coworkers[17] Cr(VI) is reduced to Cr(III) at mild reducing conditions; at the same time formation of Cr(V) or Cr(IV) was not observed. Reduction under severe conditions (temperature above 500°C) led to the formation of well dispersed zero-valent chromium with nonmetallic structure stabilized by the support. Similarly, Hurst and coworkers[18] and Mahoney, Rudham, and Summers[19] reported that reduction of Cr(III) to Cr(0) is very difficult and takes place only at high temperatures. The maximum hydrogen consumption, observed at 540°C (see Fig. 2) is in accordance with these findings.

Impregnation of supports with rhodium chloride causes an increase of hydrogen consumption during temperature-programmed reduction. TPR curves for Rh/Al_2O_3 and $Rh/(Al_2O_3 + Cr_2O_3)$ catalysts were very similar: the maximum hydrogen consumption was located at 310°C and 430°C. The smaller area below TPR curves for the Rh/Al_2O_3 catalyst indicates that part of rhodium (incorporated in the subsurface layers of Al_2O_3 during calcination) became hard to reduce[18,20]. The Rh/Cr_2O_3 catalyst was reduced in three steps at 160, 320, and 540°C. The first two steps correspond probably to the reduction of rhodium dispersed in a different way on the surface[21]. Very likely, the third reduction step corresponds to reductionof Cr(III) to Cr(0).

Number of surface OH *groups.* The dependence of the specific number of surface OH groups of the supports activated at 300, 400, and 500°C on the support composition passed always through a minimum (Fig. 3). Pure Cr_2O_3 had the highest number of OH groups whereas mixed supports the lowest. This is, obviously, connected with the activation of samples in hydrogen. Cr(VI) oxide located on the surface of mixed chromium and aluminium oxides began to be reduced below 100°C and, therefore, the number of OH groups decreased in comparison with pure Al_2O_3, which is not affected by reduction.

The increase of activation temperature from 300 to 400°C caused a marked decrease in number of surface OH groups; further increase of temperature to 500°C had, however, only a slight effect. This is well demonstrated in Fig. 4, where the specific number of surface OH groups is plotted versus reciprocal activation temperature. Similar dependence was observed by Nondek[15].

Catalyst activity and selectivity. The catalytic activity of the prepared samples of supported rhodium catalysts changed markedly with time on stream. In order to elucidate the influence of catalyst support composition we have, therefore, used as the measure of the catalyst performance the composition of reaction products obtained on fresh samples in grained form (0·3 – 0·5 mm).

The obtained results are summarized in Fig. 5; the toluene conversion, x_T, decreases slightly with increasing amount of Cr_2O_3 in the catalyst supports at constant space time ($W/F = 0{\cdot}2\ g_{cat}h/mol_T$): from 98% for Rh/Al_2O_3 to 81% for Rh/Cr_2O_3. The samples differed, however, markedly in selectivity: selectivity to benzene, S_B, was the highest for Rh/Cr_2O_3 and the lowest for Rh/Al_2O_3. Parameter $P(CH_4)$, characterizing the undesirable methane formation, was highest for Rh/Al_2O_3 and decreased with the increasing amount of Cr_2O_3 in the support; at about 35% of Cr_2O_3 in the support the methane formation would vanish and the catalyst would lose the (undesirable) hydrodealkylation and methanation activity. The high hydrogen formation

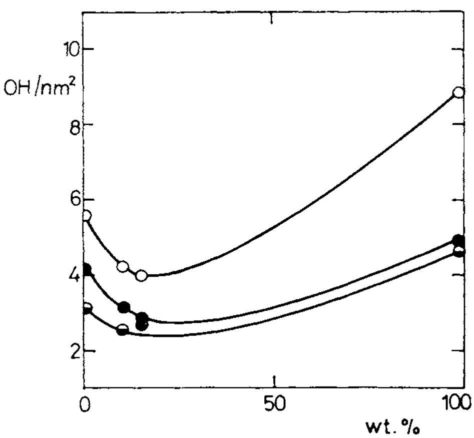

FIG. 3

Specific number of surface OH groups for supports with different amount of Cr_2O_3; activation temperature: ○ 300°C; ● 400°C; ⊖ 500°C

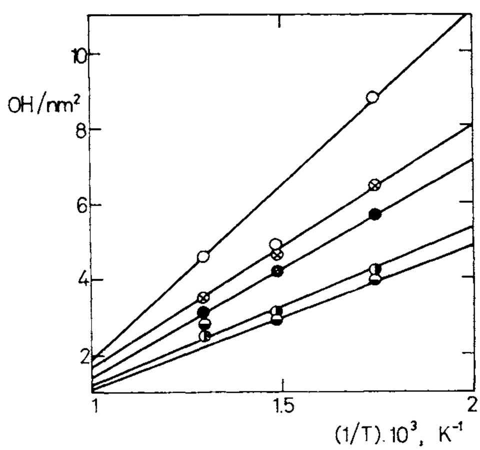

FIG. 4

Specific number of surface OH groups versus reciprocal activation temperature. Amount of Cr_2O_3 in support (wt. %): ● 0%; ◑ 10%; ⊖ 16%; ○ 100%. ⊗ data for Al_2O_3 from Nondek[15] (characterized by the parameter $P(H_2)$) for the Rh/Al_2O_3 is caused by high total decomposition of toluene and/or benzene (Eqs (5), (6)). CO_2 formation (parameter $P(CO_2)$) is lower on samples which are richer in Cr_2O_3; contrary to this, CO formation (parameter $P(CO)$) passes through a minimum and would be lowest at about 50 wt. % of Cr_2O_3 in the support.

The influence of rhodium catalyst support composition on the selectivity in toluene steam dealkylation can be also judged from the dependences of S_B and $P(i)$ on toluene conversion, x_T, in Fig. 6. It follows from the general form of these dependences that the steam dealkylation takes place through a complicated reaction network

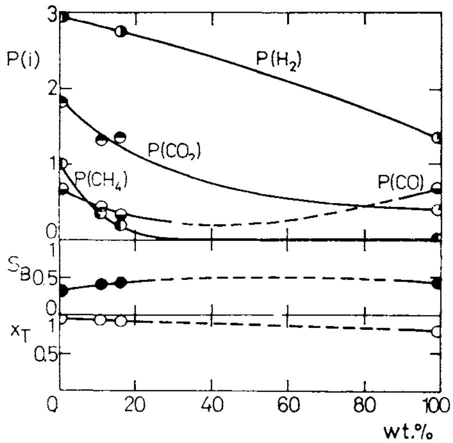

FIG. 5

Conversion of toluene, x_T, selectivity to benzene, S_B, and parameters $P(H_2)$, $P(CH_4)$, $P(CO)$, and $P(CO_2)$ for rhodium catalysts with different amount of Cr_2O_3 in the support; 460°C, 0·1 MPa, $W/F = 0{\cdot}2\ g_{cat}$ h/mol_T, molar ratio water/toluene in the feed 5/1

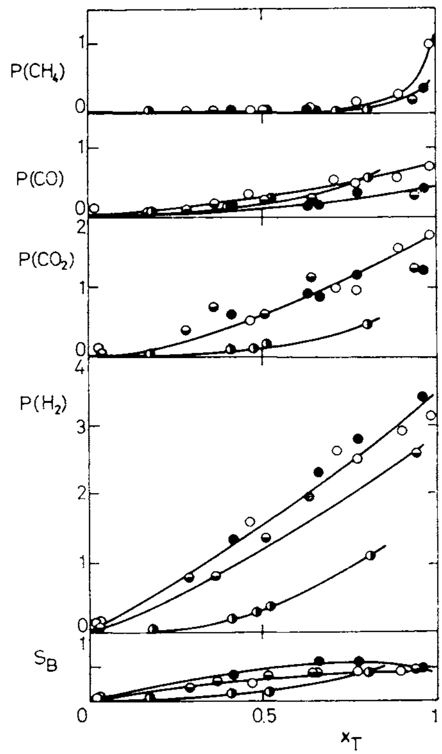

FIG. 6

Selectivity to benzene, S_B, and parameters $P(CH_4)$, $P(CO)$, $P(CO_2)$, and $P(H_2)$ for different toluene conversions; 460°C, 0·1 MPa, molar ratio water/toluene in the feed 5/1. Amount of Cr_2O_3 in the support (wt. %): ○ 0%; ● 10%; ◒ 16%; ◑ 100%

in which methane is formed by consecutive reaction steps. The dependences for all samples containing Al_2O_3 are similar and differ somewhat from those for Rh/Cr_2O_3. On all samples containing Al_2O_3, high formation of hydrogen takes place, mainly due to total toluene decomposition. This reaction is weaker when the amount of Cr_2O_3 increases. Similarly, less formation of CO and CO_2 is observed when more Cr_2O_3 is present in the sample. The highest selectivities to benzene on Al_2O_3 containing catalysts are obtained at toluene conversions of about 75%. For the Rh/Cr_2O_3 catalyst such a selectivity maximum was not detected even at $x_T = 80\%$; it is likely that on this catalyst S_B will increase with x_T above the maximum for Al_2O_3.

Molar ratios of CO_2/CO in gaseous reaction products shown in Fig. 7 characterize the significance of conversion reaction.

$$CO + H_2O \rightarrow CO_2 + H_2 \tag{3}$$

The highest value of this ratio for the Rh/Cr_2O_3 catalyst (0·75) is reached already at toluene conversion $x_T = 0{\cdot}2$. At higher x_T no increase in CO_2/CO can be observed. With catalysts containing Al_2O_3 the situation is different: the ratio CO_2/CO changes with x_T over the whole conversion interval and is always much higher (up to 4·5).

The significance of the methanization reaction is demonstrated by the molar ratio CH_4/CO of gaseous products. On Rh/Cr_2O_3 this reaction is negligible up to toluene conversion of at least 80%. On the Al_2O_3 containing catalysts methanation reaction increases steadily with toluene conversion; the differences in the amount of Al_2O_3 in the support are unimportant.

Textural properties of deactivated catalysts. Surface areas of fresh and deactivated supported rhodium catalysts are summarized in Table IV. It can be seen that the

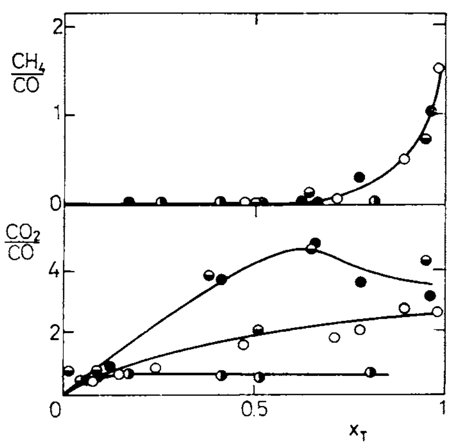

FIG. 7

Molar ratios CO_2/CO and CH_4/CO in reaction products obtained at different toluene conversions. Amount of Cr_2O_3 in the support (wt. %): ○ 0%; ● 10%; ⊖ 16%; ◑ 100%

changes are minor and can be explained by experimental errors. The same is true for pore size distributions of fresh and deactivated catalysts. Thus, the activity decrease is caused rather by blocking of catalytically active rhodium particles than by decrease of the total surface area.

TABLE IV

Specific surface areas of catalysts (m^2/g)

Cr_2O_3 in support, wt. %	Fresh catalysts	Deactivated catalysts
0	148	147
10	130	125
16	121	113

TABLE V

Initial toluene steam dealkylation rates on catalyst pellets, r_p^o, and grains r^o, and effectiveness factors $\eta = r_p^o/r^o$

Cr_2O_3 in support, wt. %	r^o s^{-1}	r_p^o s^{-1}	η_{exp}	η_{calc}
0	7·54	4·37	0·58	0·56
10	3·71	3·19	0·86	0·76
16	2·60	2·21	0·85	0·83

TABLE VI

Published rate equations for steam dealkylation of toluene

Catalyst	Temp., °C	Rate equation[a]	Ref.
RhPt/α-Al_2O_3	400–500	$r = kp_T^{0.25}p_W^{0.35}$	25
Rh/Al_2O_3	430–480	$r = kp_Tp_W/p_{CO}$	26
Rh/Al_2O_3	440–480	$r = kp_Tp_W$	27
Rh/γ-Al_2O_3	400–480	$r = kp_T/(b_Tp_T + b_{CO}p_{CO})$	28
Rh/Al_2O_3	431	$r = kp_Tp_W/(1 + b_Tp_T)(1 + b_Wp_W)$	29[b]

[a] r reaction rate; p_i partial pressure of component i (toluene i = T; water i = W); [b] initial reaction rate region (i.e. absence of products).

Effectiveness of pelleted catalysts. Initial rates of toluene steam dealkylation on supported rhodium catalysts pellets, r_p^0, and small grains, r^0, determined as slopes of the experimental kinetic curves $x_T - W/F$ at $W/F = 0$ are summarized in Table V. It is seen that due to intraparticle diffusion effects the Rh/Al_2O_3 pellets are utilized to less than 60%. Because of decreased catalytic activity and increased transport pore radii the addition of 10 or 16 wt. % of Cr_2O_3 to the catalyst support results in increase of pellet utilization to about 85%.

Prediction of pellets effectiveness factors. Characteristics of transport pores, $\bar{r}$ and ψ can be used for prediction of effectiveness factors of pelleted catalysts[22]. Such a prediction requires, however, the knowledge of rate equation for toluene steam dealkylation. Several kinetic studies were published on toluene steam dealkylation over Rh/Al_2O_3 catalysts; as can be seen from Table VI the rate equations obtained by different authors differ markedly. We have, therefore, described the reaction kinetics by simple first order rate equation $r = kp_T$; the agreement of this description with experiments is illustrated in Fig. 8 (curve *1*) for the Rh/Al_2O_3 catalyst. In view of the water/toluene molar ratio in the feed equal to 5/1 the water concentration in the reaction mixture surrounding the catalyst pellets was assumed to be constant. The prediction of pellet effectiveness factors was based on the theory of multicomponent diffusion of gases in porous media; at the same time the diffusion in the transition region between Knudsen and bulk diffusion was taken into account[23]. For this case and for Rh/Al_2O_3 catalyst pellets surrounded by 1/5 toluene/water mixture at 460°C and 0·1 MPa (initial reaction rate region) the effective diffusion coefficient of toluene in the reaction mixture was evaluated as equal to $9 \cdot 5 \, . \, 10^{-4}$ cm²/ /s. Because of the large excess of water vapour around the pellets the change of effective diffusion coefficient of toluene along the pores can be neglected (in the

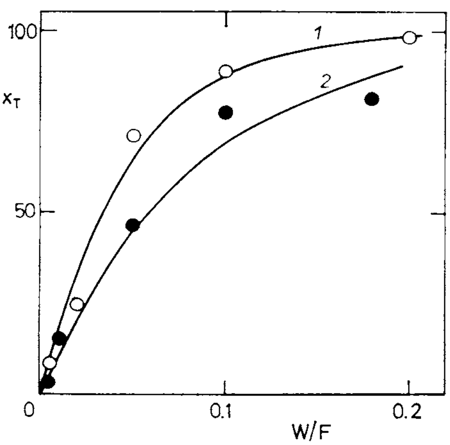

FIG. 8

Kinetic curves for toluene steam dealkylation on grains (*1*) and pellets (*2*) of Rh/Al_2O_3 catalyst (460°C, 0·1 MPa). Curves calculated, points experimental centre of pellets the effective diffusivity amounts to $9 \cdot 7 . 10^{-4}$ cm^2/s) and the pellet effectiveness factor can be easily evaluated[22]. Detailed description of the applied procedure can be found elsewhere[24].

Fig. 8 shows the calculated dependence of toluene conversion on space time for pelleted catalyst Rh/Al_2O_3 (curve 2) together with experimental points as an illustration of the good quality of the catalyst effectiveness prediction. Similar agreement was obtained also for rhodium catalysts with mixed supports. Table IV compares the calculated effectiveness factors for the initial reaction rate region. The good agreement o experimental and predicted effectiveness factors indicates the usefulness of characterizing the transport properties of porous catalysts; knowledge of transport parameters is essential for prediction of the role of intraparticle diffusion on reaction rate and selectivity on pelleted catalysts based solely on kinetic measurements in the kinetic region.

The authors are indebted to Go Yong Ul from the Institute of Chemistry, Hamhung, DPR Korea, for measurement of catalytic activities and to R. Pospěch and D. Tomanová from the Institute of Chemical Process Fundamentals, Czechoslovak Academy of Sciences, Prague, for textural measurements.

REFERENCES

1. Grenoble D. C., Estadt M. M., Ollis D. F.: J. Catal. *67*, 90 (1981).
2. Grenoble D. C. J.: J. Catal. *51*, 203 (1978).
3. Duprez D., Pereira P., Miloudi A., Maurel R.: J. Catal. *75*, 151 (1982).
4. Mozhaiko V. N., Rabinovich G. L., Maslyanskii G. N., Erdyakova L. P.: Neftekhimiya *15*, 95 (1975).
5. Duprez D., Miloudi A., Delahay G., Maurel R.: J. Catal. *90*, 292 (1984).
6. Grenoble D. C.: J. Catal. *56*, 32, 40 (1979).
7. Rabinovich G. L., Maslyanskii G. N., Treiger L. M.: Kinet. Katal. *12*, 1567 (1971).
8. Dydikina G. V., Rabinovich G. L., Maslyanskii G. N., Dementeva M. I.: Kinet. Katal. *10*, 497 (1969).
9. Rabinovich G. L., Maslyanskii G. N., Vorobev V. G., Vasilev I. A., Biryukova L. M., Ioffe I. I.: Neftekhimiya *13*, 518 (1973).
10. Treiger L. M., Rabinovich G. L., Maslyanskii G. N.: Kinet. Katal. *14*, 1582 (1973).
11. Ferino I., Marongin B., Torazza S., Forni L.: React. Kinet. Catal. Lett. *15*, 95 (1980).
12. Duprez D., Miloudi A., Delahay G., Maurel R.: J. Catal. *101*, 56 (1986).
13. Kochloefl K.: *Proc. 6th Internat. Congr. Catalysis London, 1976*. Chem. Soc., London 1977.
14. Petrini G., Fott P., Schneider P.: Collect. Czech. Chem. Commun. *48*, 215 (1983).
15. Nondek L.: React. Kinet. Catal. Lett. *2*, 283 (1975).
16. Satterfield C. N.: *Mass Transfer in Heterogenous Catalysis*. MIT Press, Cambridge (Mass.) 1970.
17. Grünert W., Shapiro E. S., Feldhaus R., Anders K., Antoshin G. V., Minachev Kh. M.: J. Catal. *100*, 138 (1986).
18. Hurst N. W., Gentry S. J., Jones A., McNicol B. D.: Catal. Rev. Sci. Eng. *24*,233 (1982).
19. Mahoney F., Rudham R., Summers J. V.: J. Chem. Soc., Faraday Trans. 1, *75*, 314 (1979).
20. Jao H. C., Japar S., Shelef M.: J. Catal. *50*, 407 (1977).

21. Vis J. C., van't Blick H. F. J., Huizinga T., van Grondelle J., Prins R.: J. Catal. *95*, 333 (1985).
22. Schneider P.: Chem. Eng. Commun. *2*, 155 (1976).
23. Schneider P.: Chem. Eng. Commun. *1*, 239 (1974).
24. Petrini G., Schneider P.: Chem. Eng. Sci. *39*, 637 (1984).
25. Kasaoka S., Omoto M., Watanabe T., Tokamatsu K.: Nippon Kagaku Kaishi *1978*, 1418.
26. Grigoreva L. N., Slovokhotova T. A.: Neftekhimiya *11*, 842 (1971).
27. Grigoreva L. N., Maslyanskii G. N., Rabinovich G. L., Slovokhotova T. A.: Neftekhimiya *12*, 195 (1972).
28. Vorobev V. S., Pilyavskii V. P., Dorokhov A. P., Treiger L. M.: Internat. Chem. Eng. *15*, 611 (1975).
29. Beltramo P., Ferino I., Forni L., Torrazza S.: Chim. Ind. (Milano) *60*, 191 (1978).

Translated by the author (K.J.).